

# Tunability of Fluorescent Metal-Organic Frameworks through Dynamic Spacer Installation with Multivariate Fluorophores

Cheng-Xia Chen, Qian-Feng Qiu, Mei Pan, Chen-Chen Cao, Neng-Xiu Zhu, Hai-Ping

Wang, Ji-Jun Jiang, Zhang-Wen Wei\*, Cheng-Yong Su\*

*MOE Laboratory of Bioinorganic and Synthetic Chemistry, Lehn Institute of Functional materials, School of Chemistry, Sun Yat-Sen University, Guangzhou 510275, China.*

<a href="#">S1.</a>	<a href="#">Materials and Instrumentation</a>	2
<a href="#">S2.</a>	<a href="#">Ligand Synthesis</a>	3
<a href="#">S3.</a>	<a href="#">MOF Synthesis</a>	6
<a href="#">S4.</a>	<a href="#">Single Crystal X-Ray Crystallography</a>	7
<a href="#">S5.</a>	<a href="#">Powder X-ray Diffraction</a>	10
<a href="#">S6.</a>	<a href="#">Sample Preparation and Excitation Spectra</a>	13
<a href="#">S7.</a>	<a href="#">Variable-Temperature-Dependent Powder X-Ray Diffraction</a>	14
<a href="#">S8.</a>	<a href="#"><sup>1</sup>H NMR Spectroscopy</a>	17
<a href="#">S9.</a>	<a href="#">N<sub>2</sub> Sorption Isotherm</a>	20
<a href="#">S10.</a>	<a href="#">Dynamic Reversible Ligand Installation</a>	23
<a href="#">S11.</a>	<a href="#">Microscopic Photos</a>	30
<a href="#">S12.</a>	<a href="#">PXRD, UV-Vis Spectra and Fluorescent Spectra of Reinstalled MOFs</a>	33
<a href="#">S13.</a>	<a href="#">Reference</a>	33

## S1. Materials and Instrumentation

All the reagents and solvents were purchased from commercial sources and directly utilized without further purification. Anthracene-9-carboxylic acid ( $\text{H}_2\text{L}^2$ ), 1-naphthoic acid ( $\text{H}_2\text{L}^4$ ), 1,4-naphthalenedicarboxylic acid ( $\text{H}_2\text{L}^5$ ), and 2,6-naphthalenedicarboxylic acid ( $\text{H}_2\text{L}^6$ ) were purchased commercially from ENERGY CHEMICAL. Solid-state IR spectra were recorded using Nicolet/Nexus-670 FT-IR spectrometer in the region of 4000-400  $\text{cm}^{-1}$  using KBr pellets. Single crystal X-ray diffraction data were collected on an Agilent Technologies SuperNova X-RAY diffractometer system equipped with a Cu sealed tube ( $\lambda = 1.54178$ ) at 50 kV and 0.80 mA. Powder X-ray diffraction (PXRD) was carried out with a RigakuSmartLab diffractometer (Bragg-Brentano geometry, Cu  $\text{K}\alpha 1$  radiation,  $\lambda = 1.54056$  Å), or a Rigaku MiniFlex600 diffractometer (Bragg-Brentano geometry, Cu  $\text{K}\alpha 1$  radiation,  $\lambda = 1.54056$  Å). Thermogravimetric analyses (TGA) were performed on a NETZSCH TG209 system in nitrogen and under 1 atm of pressure at a heating rate of 10  $^\circ\text{C min}^{-1}$ . Nuclear magnetic resonance (NMR) data were collected on a 400 MHz Nuclear Magnetic Resonance Spectrometer. UV-Vis absorption spectra were recorded using a Shimadzu UV-2450 spectrophotometer. Fluorescence microscopy photos were taken by UV lamp using 350/50 nm Excitation Filter and 420/ $\infty$  nm Barrier Filter. Fluorescence spectra were measured by Edinburgh FLS 980 spectrometer. Gas adsorption isotherms for pressures in the range of 0-1.0 bar were obtained by a volumetric method using a quantachrome autosorb-iQ2-MP gas adsorption analyzer. Gas adsorption measurements were performed using ultra-high purity  $\text{N}_2$  gas. The absolute quantum yields for fluorescence emission (400 to 800 nm) were measured with a quartz sample holder in an integrating sphere attached to the EDINBURGA FLS980 spectrophotometer. The overall quantum yield  $\Phi$  is calculated by

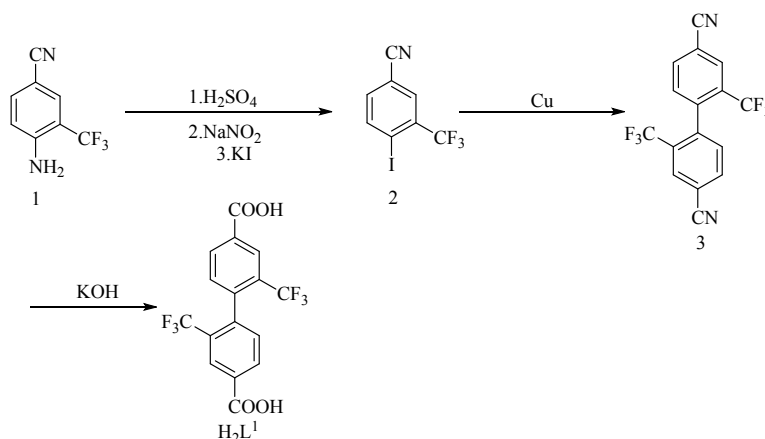
$$\Phi = S(\text{Em}) S(\text{Abs}) = \frac{\int \lambda hc [I_{\text{sample}}(\text{em})(\lambda) - I_{\text{reference}}(\text{em})(\lambda)] d\lambda}{\int \lambda hc [I_{\text{sample}}(\text{ex})(\lambda) - I_{\text{reference}}(\text{ex})(\lambda)] d\lambda}$$

Where  $S(\text{Em})$  means the number of photons emitted from the sample;  $S(\text{Abs})$  means the number of photons absorbed by the sample;  $\lambda$  means the wavelength;  $h$  means Planck's constant;  $c$  means the velocity of light;  $I_{\text{sample}}(\text{em})$  and  $I_{\text{reference}}(\text{em})$  mean the photoluminescence intensities with and without the sample, respectively;  $I_{\text{sample}}(\text{ex})$  and

$I_{\text{reference(ex)}}$  mean the integrated intensities of excitation light with and without a sample, respectively.

## S2. Ligand Synthesis

### 2.1 2, 2'-Bis(trifluoromethyl)-4,4'-biphenyldicarboxylic acid ( $\text{H}_2\text{L}^1$ )



**Scheme S1** Synthetic path for organic linker  $\text{H}_2\text{L}^1$ .

The ligand  $\text{H}_2\text{L}^1$  was prepared using a modified literature procedure:<sup>1</sup>

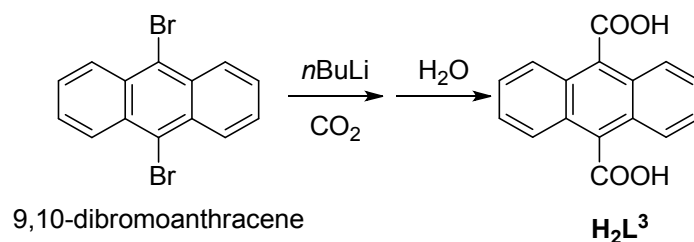
2-Amino-5-cyanobenzotrifluoride (1) (5.00 g, 26.86 mmol), concentrated sulfuric acid (20 mL), water (14 mL) and a magnetic stir bar were added to a 250-mL three-neck flask. After the reaction mixture became clear, it was cooled to 0 °C with ice bath. A solution of sodium nitrite (2.20 g, 31.87 mmol) in water (4.5 mL) was added dropwise to the reaction mixture while the temperature was maintained below 3 °C. The reaction mixture was further stirred at 0 °C for 1 h, and then filtrated to obtain the clear filtrate. A solution of potassium iodide (6.30 g, 37.95 mmol) in water (111 mL) was slowly added to the resulted diazonium salt filtrate with vigorous stirring at 0 °C. After the addition, the reaction mixture was left under stirring at 0 °C for 1 h. Then the mixture was allowed to warm to room temperature. The precipitate that formed was collected and washed with dilute sodium bisulfate aqueous solution and water. The precipitate was purified by silica column chromatography (20:1 petroleum ether/ethyl acetate) to obtain white solid (4.53 g, yield: 56.7%):  $^1\text{H}$  NMR( $\text{CDCl}_3$ , 400MHz):  $\delta$  7.50 (d, 1H,  $J$  = 8.2, Ar-H), 7.91 (d, 1H,  $J$  = 1.8, Ar-H), 8.22 (d, 1H,  $J$  = 8.2, Ar-H);  $^{19}\text{F}$  NMR ( $\text{CDCl}_3$ , 400MHz):  $\delta$  63.59.

Copper powder (20 g) was treated with a 2% solution of iodine in acetone (200 mL) at room temperature for 30 min. The copper powder was collected by filtration and washed thoroughly with 1:1 acetone/concentrated hydrochloric acid solution (100 mL). The copper powder was again collected by filtration and washed with acetone until pH of the filtrate reach 7, and then dried under reduced pressure at 60 °C for 24 h.

5-Cyano-2-iodobenzotrifluoride (2) (4.00 g, 13.70 mmol), activated copper (8.00 g, 125.88 mmol) and N,N-dimethylformamide (DMF) (8 mL) were mixed under N<sub>2</sub> atmosphere and then heated to 155 °C and kept for 10 h. After the reaction mixture was filtered while it was still hot, the filtrate was collected and poured into water (100 mL) and stirred vigorously. The formed precipitate was collected by filtration and dried under reduced pressure at 60 °C overnight to afford white solid (1.8 g, yield: 78.26%). <sup>1</sup>H NMR (CDCl<sub>3</sub>, 400MHz): δ 7.47 (d, 2H, *J* = 5.2, Ar-H), 7.93 (d, 2H, *J* = 5.8, Ar-H), 8.05 (d, 2H, Ar-H); <sup>19</sup>F NMR(CDCl<sub>3</sub>, 400MHz): δ 58.65.

2,2'-Bis(trifluoromethyl)-4,4'-biphenyldicarbonyl (3) (1.50 g, 4.41 mmol), potassium hydroxide (1.08 g, 19.25 mmol), diethylene glycol (10 mL) and water (0.33 mL) were added to a 100 mL one-neck flask equipped with a condenser and a magnetic stirrer. The reaction mixture was heated at 165 °C overnight. After the reaction mixture was allowed to cool to room temperature, water (80 mL) was added. After the solution was filtered, the clear filtrate was acidified with concentrated hydrochloric acid until its pH reach 1. The precipitate that formed was collected by filtration, washed with water and dried under reduced pressure at 60 °C for 24 h to afford white solid (1.43 g, yield: 85.63 %): <sup>1</sup>H NMR (d<sup>6</sup>-DMSO, 400 MHz): δ 7.59 (d, 2H, *J* = 8.0, Ar-H), 8.27 (dd, 2H, *J* = 8.0, 1.3, Ar-H), 8.31 (d, 2H, *J* = 1.2, Ar-H), 13.74 (s, 2H, -COOH); <sup>13</sup>C NMR (d<sup>6</sup>-DMSO, 400 MHz): δ 166.15, 140.41, 132.69, 132.49, 132.35, 126.97, 125.09, 122.41; <sup>19</sup>F NMR (d<sup>6</sup>-DMSO, 400 MHz): δ 57.31. ESI-MS: *m/z* calcd for C<sub>16</sub>H<sub>6</sub>F<sub>6</sub>O<sub>4</sub><sup>2-</sup> 376.02, found 376.96. FTIR (KBr): ν = 2892 (m), 2663 (w), 2568 (w), 1705 (s), 1615 (m), 1574 (w), 1438 (m), 1406 (m), 1320 (s), 1276 (s), 1171 (m), 1130 (s), 1073 (m), 1004 (w), 926 (m), 859 (w), 777 (w), 757 (w), 685 (m), 543 (w) cm<sup>-1</sup>.

## 2.2 Anthracene-9, 10-dicarboxylic acid (H<sub>2</sub>L<sup>3</sup>)



**Scheme S2** Synthetic path for organic linker **H<sub>2</sub>L<sup>3</sup>**.

The ligand **H<sub>2</sub>L<sup>3</sup>** was prepared using a modified literature procedure.<sup>2</sup> 2.004 g of 9,10-dibromoanthracene was mixed with 8.1 mL of 1.6 M *n*BuLi in dry ether at 0 °C for 2 h. To the resulting orange mixture was added 0.3 g of dry ice at -78 °C. The entire reaction was allowed to proceed for about 10 h before working up with water and hydrochloric acid. The bright yellow precipitate was collected (1.11 g, yield: 70 %). <sup>1</sup>H NMR (d<sup>6</sup>-DMSO, 400 MHz): δ 7.69 (dd, 4H, *J* = 6.9, Ar-H), 8.07 (dd, 4H, *J* = 6.8, 1.3, Ar-H).

## S3. MOF Synthesis

### 3.1 Synthesis of LIFM-28

LIFM-28 were prepared using a modified literature procedure.<sup>1</sup> ZrCl<sub>4</sub> (100 mg, 0.40 mmol), H<sub>2</sub>L<sup>1</sup> (140 mg, 0.37 mmol), trifluoroacetic acid (1.0 mL, 13.46 mmol) and DMF (20 mL) were added into a vial. The mixture was heated in a 120 °C oven for 72 h. Then the reaction mixture was cooled to 30 °C at a rate of 10 °C / 100 min. The colorless crystals formed were collected by filtration and washed with clean DMF for several times. In order to remove unreacted linkers and salts in framework channels, the as-grown crystals were soaked in DMF (20 mL) at 85 °C for 24 h. After cooling to room temperature, the solid was obtained by centrifugation. Then the solid was soaked in methanol (MeOH) for 2 d during which the solvent was decanted and freshly replenished every 24 h. After 2 d of soaking, the crystals were isolated via centrifugation at 10,000 rpm for 5 min in a fixed-angle rotor, followed by drying under vacuum (93 mg, yield: 53.4 %). FTIR (KBr):  $\nu$ = 3428 (s), 1611 (s), 1550 (m), 1436 (s), 1395 (s), 1309 (s), 1182 (m), 1127 (s), 1073 (m), 1005 (w), 927 (w), 783 (m), 655 (m), 542 (w), 455 (m) cm<sup>-1</sup>. Anal. calc. for [Zr<sub>3</sub>O<sub>2</sub>(OH)<sub>4</sub>(H<sub>2</sub>O)<sub>2</sub>(C<sub>16</sub>H<sub>6</sub>F<sub>6</sub>O<sub>4</sub>)<sub>2</sub>]·2MeOH·3H<sub>2</sub>O: C 31.90, H 2.68. Found: C 31.89, H, 2.61.

### 3.2 Synthesis of LIFM-31

LIFM-28 and LIFM-31 were prepared using a modified literature procedure.<sup>1</sup> LIFM-28 (10 mg, ~ 0.0043 mmol), H<sub>2</sub>L<sup>4</sup> (1.1 mg, 0.0052 mmol) and DMF (1.0 mL) were added into a vial. The mixture was heated in a 75 °C oven for 24 h. After cooling to room temperature, the crystals of LIFM-31 were collected by filtration and soaked in DMF (5 mL) at 85 °C for 24 h, and finally washed with DMF for three times (10.1 mg, yield: 95.3 %). FTIR (KBr):  $\nu$  3433 (m), 1614 (s), 1432 (s), 1391 (s), 1307 (m), 1176 (m), 1120 (s), 1072 (m), 779 (w), 656 (m), 461 (m) cm<sup>-1</sup>.

### 3.2 Synthesis of LIFM-50

LIFM-28 (10 mg), H<sub>2</sub>L<sup>2</sup> (10 mg) and DMF (2.0 mL) were charged in a vial. The mixture was heated in a 75 °C oven for 30 h. The crystals were washed with DMF

(3×), soaked in DMF (5 mL) at 85 °C for 24 h, and finally washed with DMF again (3×) (11.3 mg). FTIR (KBr):  $\nu$ = 2931 (w), 1656 (s), 1598 (m), 1559 (w), 1492 (w), 1433 (m), 1385 (s), 1304 (m), 1280 (m), 1255 (w), 1170 (w), 1118 (s), 1092 (s), 1071 (m), 1057 (m), 1006 (w), 927 (w), 886 (w), 865 (w), 782 (m), 759 (w), 735 (m), 657 (s), 636 (w), 542 (w)  $\text{cm}^{-1}$ .

### 3.3 Synthesis of LIFM-51

LIFM-28 (10 mg),  $\text{H}_2\text{L}^3$  (1.4 mg) and DMF (2.0 mL) were charged in a vial. The mixture was heated in a 75 °C oven for 30 h. The crystals were washed with DMF (3×), soaked in DMF (5 mL) at 85 °C for 24 h, and finally washed with DMF again (3×) (10.2 mg). FTIR (KBr):  $\nu$ = 3458 (w), 2931 (w), 1656 (s), 1612 (m), 1597 (m), 1560 (w), 1497 (w), 1430 (m), 1385 (s), 1305 (m), 1256 (m), 1172 (w), 1119 (s), 1091 (s), 1071 (m), 1057 (m), 1006 (w), 927 (w), 899 (w), 864 (w), 780(w), 762 (m), 733 (w), 718 (m), 695 (s), 650 (s), 571 (w)  $\text{cm}^{-1}$ .

### 3.4 Synthesis of LIFM-52

LIFM-28 (10 mg),  $\text{H}_2\text{L}^4$  (10 mg) and DMF (2.0 mL) were charged in a vial. The mixture was heated in a 75 °C oven for 30 h. The crystals were washed with DMF (3×), soaked in DMF (5 mL) at 85 °C for 24 h, and finally washed with DMF again (3×) (11.8 mg). FTIR (KBr):  $\nu$ = 2929 (w), 2861 (w), 1658 (s), 1600 (m), 1559 (w), 1504 (w), 1428 (m), 1384 (s), 1305 (m), 1282 (m), 1255 (w), 1172 (w), 1117 (s), 1090 (s), 1071 (m), 1057 (m), 926 (w), 865 (w), 784 (m), 717 (w), 695 (m), 657 (s), 590 (w)  $\text{cm}^{-1}$ .

### 3.5 Synthesis of LIFM-53

LIFM-28 (10 mg),  $\text{H}_2\text{L}^5$  (1.1 mg) and DMF (2.0 mL) were charged in a vial. The mixture was heated in a 75 °C oven for 30 h. The crystals were washed with DMF (3×), soaked in DMF (5 mL) at 85 °C for 24 h, and finally washed with DMF again (3×) (8.8 mg). FTIR (KBr):  $\nu$ = 2930 (w), 2861 (w), 1658 (s), 1598 (m), 1561 (w), 1501 (w), 1429 (m), 1384 (s), 1305 (m), 1282 (m), 1255 (w), 1174 (w), 1118 (s), 1090 (s), 1071 (m), 1057 (m), 1006 (w), 900 (w), 865 (m), 781 (m), 695 (m), 682 (w), 653 (s), 569 (w)  $\text{cm}^{-1}$ .

## S4. Single Crystal X-Ray Crystallography

Single crystals of LIFM-51 and LIFM-53 were carefully picked and coated in paratone oil, attached to a glass silk which was inserted in a stainless steel stick, then quickly transferred to the Agilent Gemini S Ultra CCD Diffractometer with the Enhance X-ray Source of Cu radiation ( $\lambda = 1.54178 \text{ \AA}$ ) using the  $\omega$ - $\phi$  scan technique. All of the structures were solved by direct methods and refined by full-matrix least squares against  $F^2$  using the SHELXL programs.<sup>3</sup> Hydrogen atoms were placed in geometrically calculated positions and included in the refinement process using riding model with isotropic thermal parameters:  $\text{Uiso}(\text{H}) = 1.2 \text{ Ueq}(-\text{CH})$ . All the electrons of disordered solvent molecules which cannot be determined, are removed by

SQUEEZE routine of PLATON program.<sup>4</sup> Crystal and refinement parameters are listed in Table S1.

#### **4.1 Note for LIFM-51 Refinement**

The trifluoromethyl groups (-CF<sub>3</sub>s) are disordered in both sides of the phenyl rings. Thus the occupancy of C8, F1, F2, F3, and H6 was refined as 59.52%, while the occupancy of other set of atoms was 40.48 %. The anthracene ring is disordered in two positions, so the occupancy of C9 and C10 was set to be 25 %, while that of C11 C12 C13 H12 H13 was set to be 50 %. O4 is highly ordered in 8 positions and its occupancy was set to be 25 %. AFIX, DFIX and SADI were used to restrain the atoms. ISOR, DELU and SIMU were used to restrain the ADP refinement. The large pores contain highly disordered solvent molecules which cannot be determined. SQUEEZE treatment was applied and the squeezed void volume is 4479 Å<sup>3</sup>, equivalent to 50.7 % of the unit cell. The R<sub>1</sub> value is 0.1161 without SQUEEZE treatment and 0.0968 with SQUEEZE treatment.

#### **4.2 Note for LIFM-53 Refinement**

The trifluoromethyl groups (-CF<sub>3</sub>s) are disordered in both sides of the phenyl rings. Thus the occupancy of C8, F1, F2, F3, and H6 was refined as 67.53 %, while the occupancy of other set of atoms was 32.47 %. The carboxylates of naphthalene ring are disordered in two positions, hence the occupancy of O3, O4, O5, C9 and H10 was set to be 25 %. AFIX, DFIX and SADI were used to restrain the atoms. ISOR, DELU and SIMU were used to restrain the ADP refinement. The large pores contain highly disordered solvent molecules which cannot be determined. SQUEEZE treatment was applied and the squeezed void volume is 5084 Å<sup>3</sup>, equivalent to 57.4 % of the unit cell. The R<sub>1</sub> value is 0.1317 without SQUEEZE treatment and 0.1056 with SQUEEZE treatment.



**Table S1** Crystallographic data for LIFM-51, LIFM-53 and LIFM-31<sup>1</sup>.

<b>Compound</b>	<b>LIFM-51</b>	<b>LIFM-53</b>	<b>LIFM-31</b>
CCDC	1850736	1850735	1474371
<i>Formula</i>	C <sub>80</sub> H <sub>32</sub> F <sub>24</sub> O <sub>34</sub> Zr <sub>6</sub>	C <sub>76</sub> H <sub>30</sub> F <sub>24</sub> O <sub>34</sub> Zr <sub>6</sub>	C <sub>76</sub> H <sub>30</sub> F <sub>24</sub> O <sub>32</sub> Zr <sub>6</sub>
<i>Formula Weight</i>	2540.37	2490.32	2458.32
<i>Shape / Color</i>	Block / Pale Yellow	Block / Colorless	Block/ Colorless
<i>Crystal System</i>	Tetragonal	Tetragonal	Tetragonal
<i>Space Group</i>	<i>P4<sub>2</sub>/mmc</i>	<i>P4<sub>2</sub>/mmc</i>	<i>P4<sub>2</sub>/mmc</i>
<i>T</i> (K)	150(2)	150(2)	173(2)
<i>a</i> (Å)	24.3839(2)	24.3097(5)	23.7851(10)
<i>b</i> (Å)	24.3839(2)	24.3097(5)	23.7851(10)
<i>c</i> (Å)	14.8719(5)	14.9770(5)	16.8399(2)
<i>α / β / γ</i> (°)	90.0 / 90 / 90	90.0 / 90 / 90	90.0 / 90.0 / 90.0
<i>V</i> (Å <sup>3</sup> )	8842.5(3)	8850.8(5)	9526.85(14)
<i>Z</i>	2	2	2
<i>D</i> <sub>calc</sub> (g/cm <sup>3</sup> )	0.954	0.934	0.857
<i>μ</i> /mm <sup>-1</sup>	3.422	3.411	3.156
<i>F</i> (000)	2480	2428	2396
<i>R</i> <sub>int</sub>	0.0572	0.0767	0.0354
<i>Reflections collected / unique</i>	16635 / 4091	15851 / 4050	28506 / 4407
<i>Completeness to theta</i>	98.3 %	96.9 %	99.3 %
<i>Data / Restraints / parameters</i>	4091 / 282 / 243	4050 / 276 / 221	4407 / 225/ 191
<i>R</i> <sub>1</sub> [ <i>I</i> >2σ( <i>I</i> )]	0.0968	0.1059	0.0579
<i>wR</i> <sub>2</sub> [ <i>I</i> >2σ( <i>I</i> )]	0.2707	0.2901	0.1628
<i>R</i> <sub>1</sub> (all data)	0.1168	0.1261	0.0619
<i>wR</i> <sub>2</sub> (all data)	0.2901	0.3150	0.1668
<i>GOF</i>	1.109	1.054	1.066

## S5. Powder X-ray Diffraction

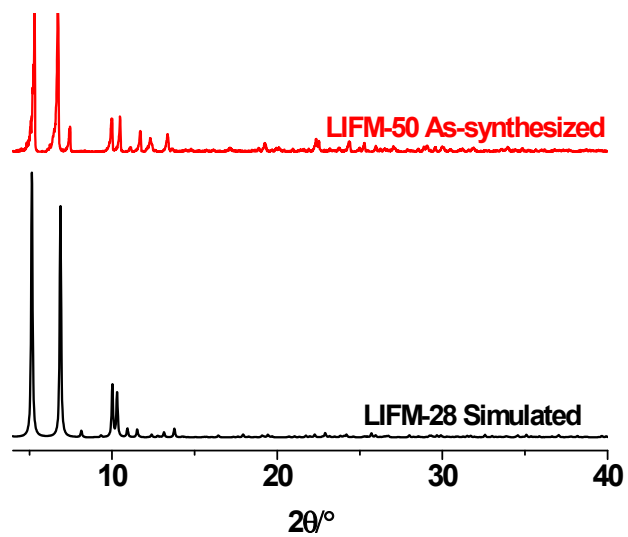


**Figure S1** The PXRD patterns of LIFM-50.

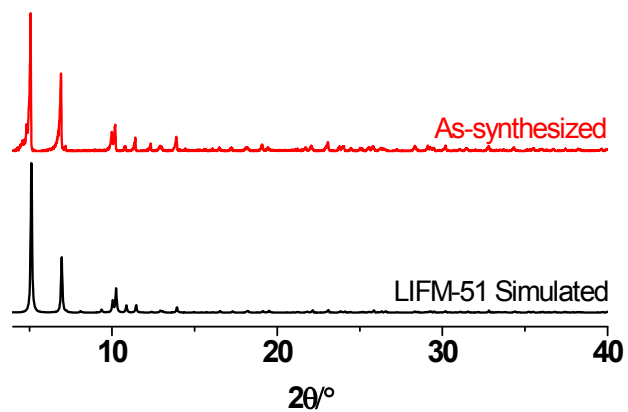


**Figure S2** The PXRD patterns of LIFM-51.

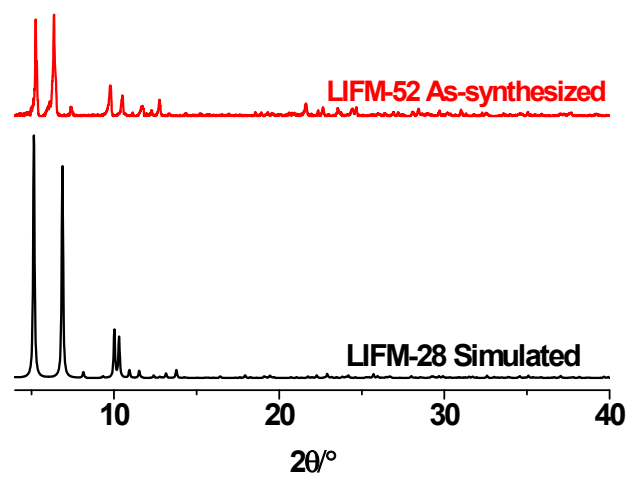


**Figure S3** The PXRD patterns of LIFM-52.

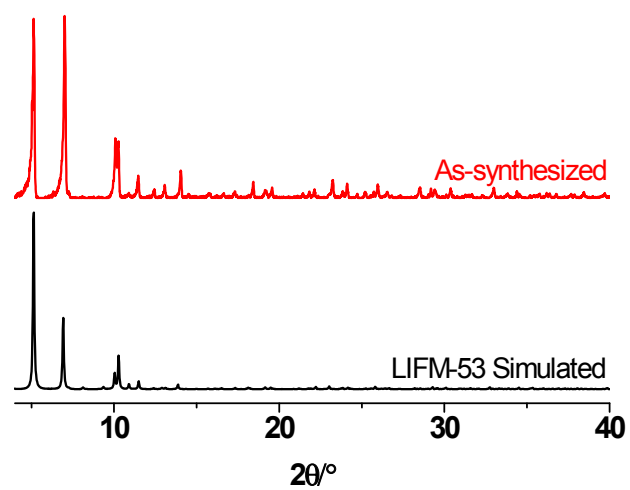


**Figure S4** The PXRD patterns of LIFM-53.

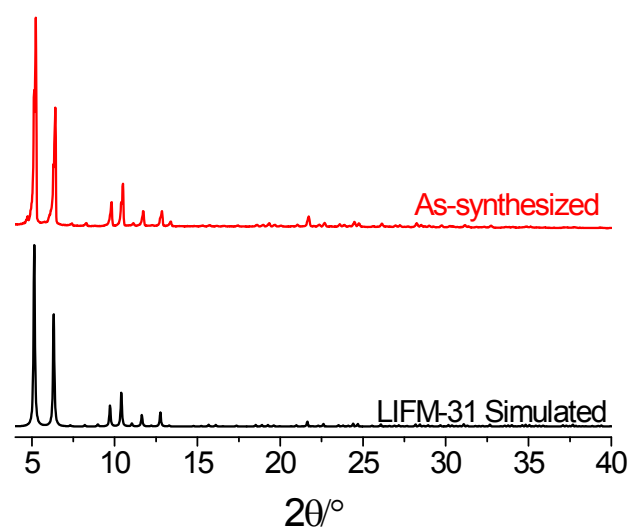


**Figure S5** The PXRD patterns of LIFM-31.

## S6. Sample Preparation and Excitation Spectra

Sample preparation:

1. MOF samples are the same activated MOF powders as samples for gas adsorption measurements. Please find the detailed procedures at section S9.
2. The powders of purchased/synthesized organic ligand precursor samples are directly used for all the fluorescent property measurements.

Excitation:

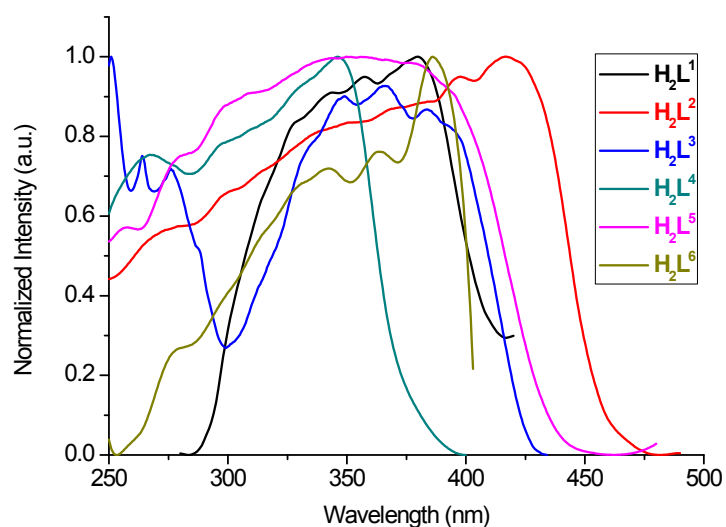


**Figure S6** The excitation spectra of  $H_2L^1$  monitored at 380 nm,  $H_2L^2$  monitored at 510 nm,  $H_2L^3$  monitored at 468 nm,  $H_2L^4$  monitored at 419 nm,  $H_2L^5$  monitored at 500 nm and  $H_2L^6$  monitored at 385 nm.

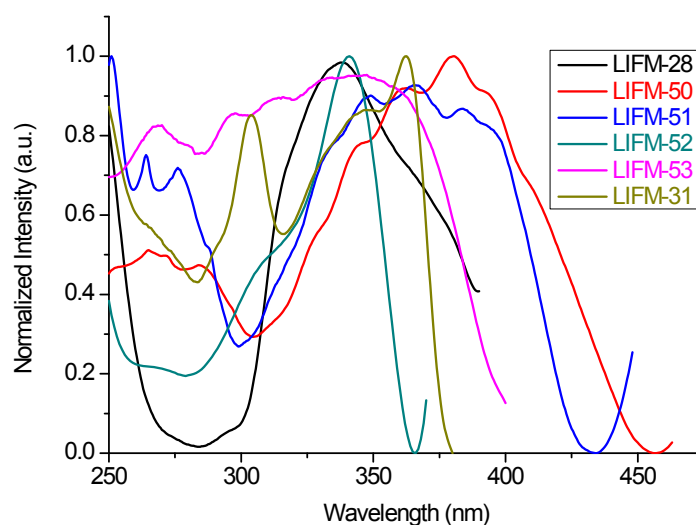


**Figure S7** The excitation spectra of LIFM-28 monitored at 410 nm, LIFM-50 monitored at 420 nm, LIFM-51 monitored at 384 nm, LIFM-52 monitored at 482 nm, LIFM-53 monitored at 468 nm and LIFM-31 monitored at 398 nm.

## S7. Variable-Temperature-Dependent Powder X-Ray Diffraction

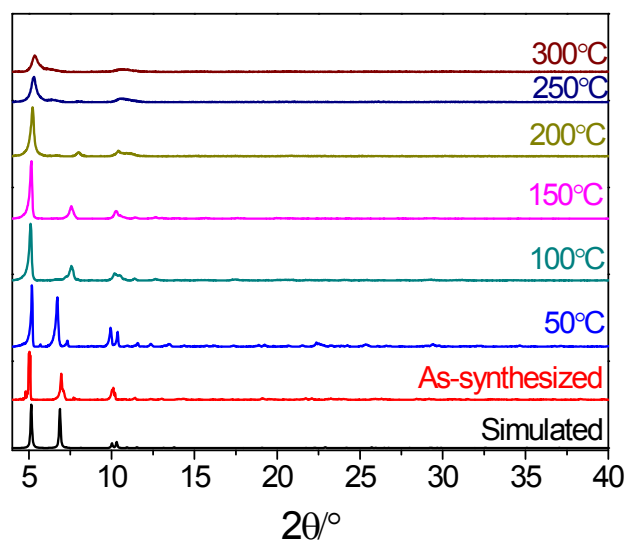


**Figure S8** Variable-temperature-dependent PXRD patterns under air atmosphere of LIFM-28.

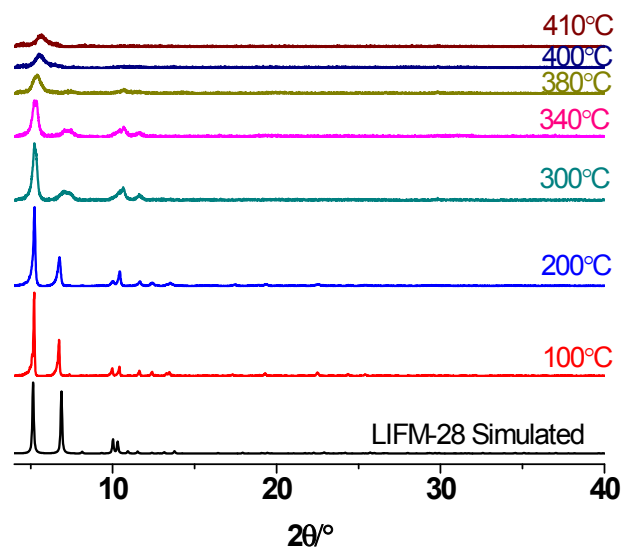


**Figure S9** Variable-temperature-dependent PXRD patterns under air atmosphere of LIFM-50.

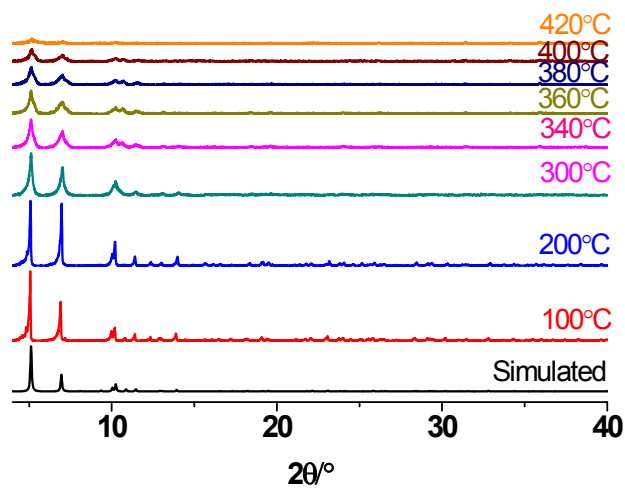


**Figure S10** Variable-temperature-dependent PXRD patterns under air atmosphere of LIFM-51.

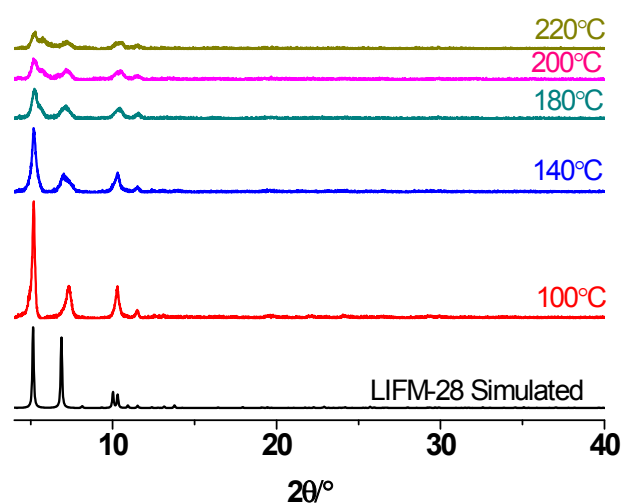


**Figure S11** Variable-temperature-dependent PXRD patterns under air atmosphere of LIFM-52.

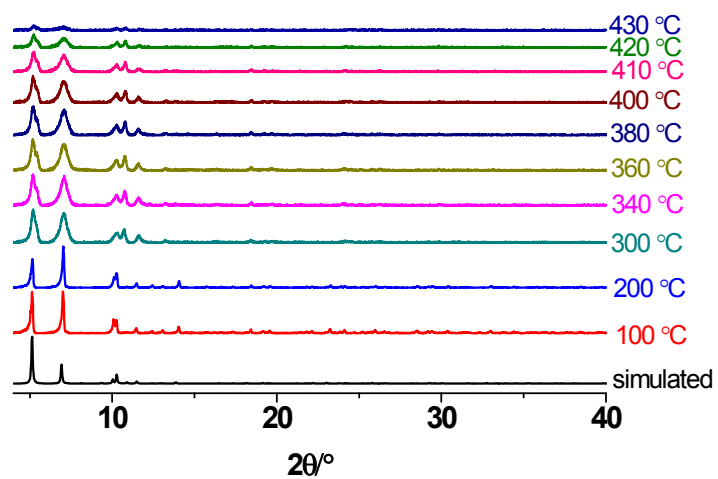


**Figure S12** Variable-temperature-dependent PXRD patterns under air atmosphere of LIFM-53.



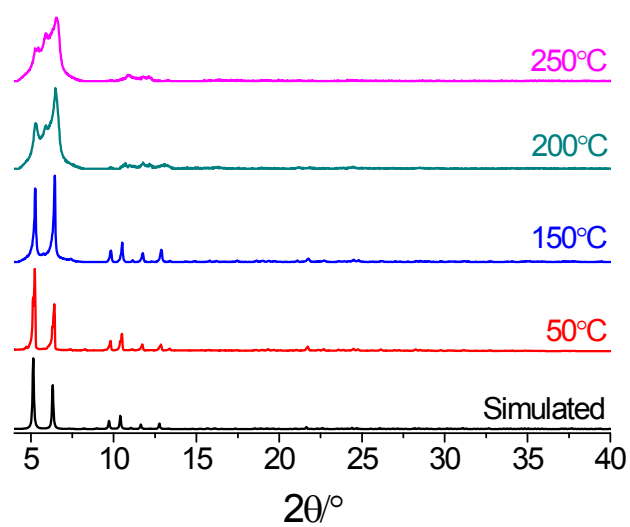


**Figure S13** Variable-temperature-dependent PXRD patterns under air atmosphere of LIFM-31.

## S8. $^1\text{H}$ NMR Spectroscopy

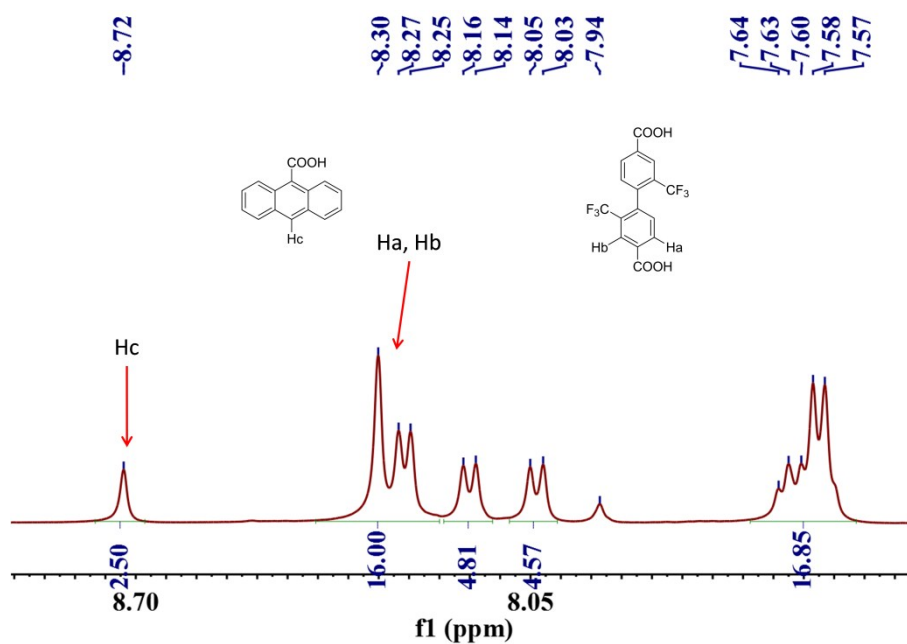


**Figure S14** The  $^1\text{H}$  NMR spectroscopy of digested LIFM-50.

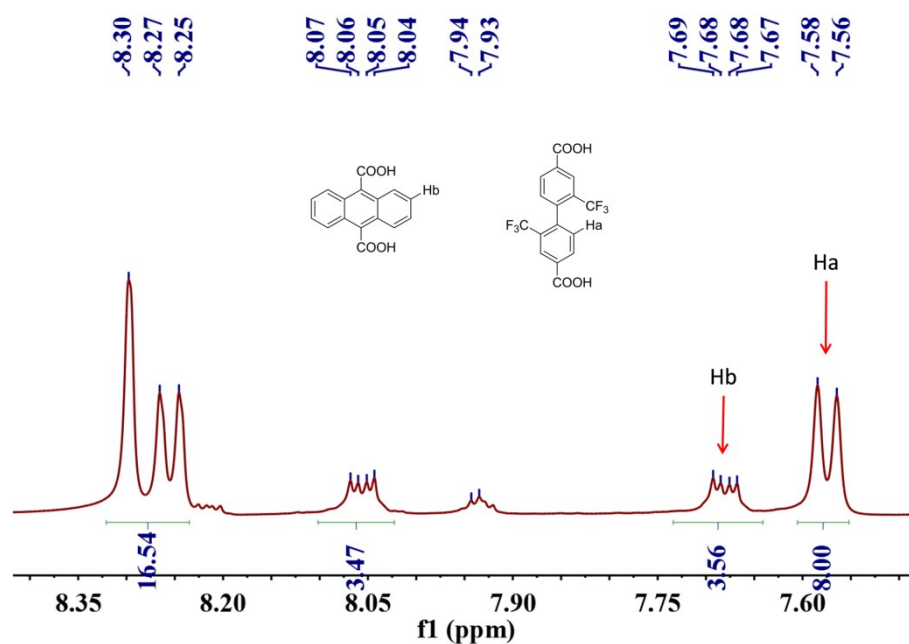


**Figure S15** The <sup>1</sup>H NMR spectroscopy of digested LIFM-51.

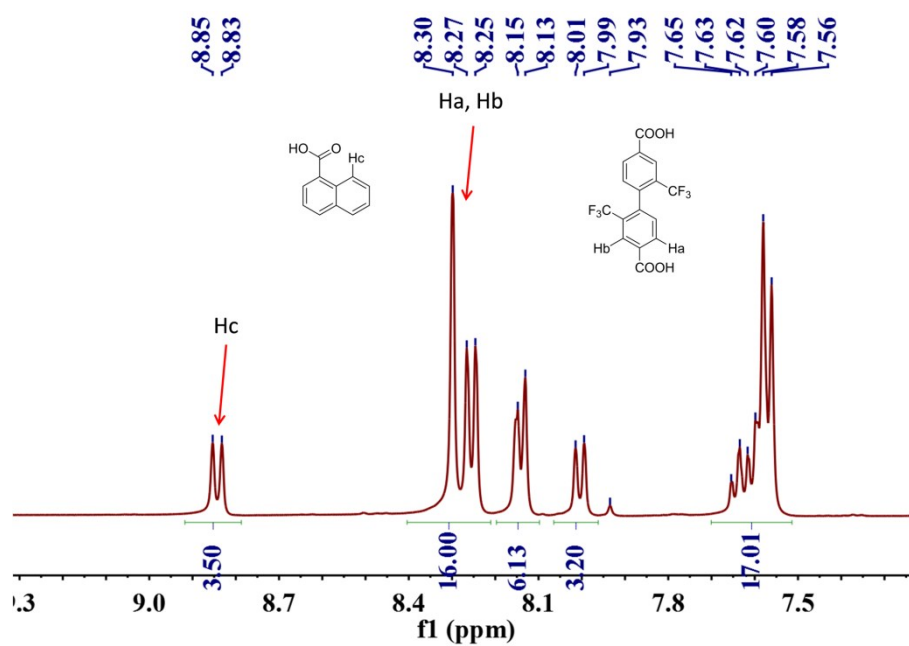


**Figure S16** The <sup>1</sup>H NMR spectroscopy of digested LIFM-52.

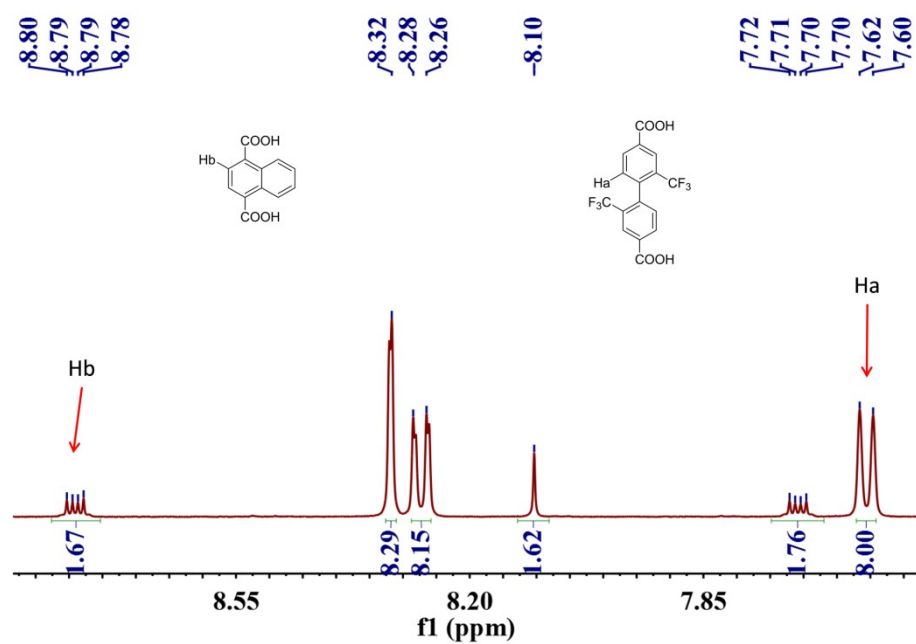


**Figure S17** The  $^1\text{H}$  NMR spectroscopy of digested LIFM-53.

**Table S2** Comparison of spacer ratios from single crystal structure and from  $^1\text{H}$  NMR of digested samples.

MOF	Spacer ratios from single crystal structure	Spacer ratios from $^1\text{H}$ NMR and $^{19}\text{F}$ NMR of digested samples <sup>a</sup>
LIFM-50	---	$\text{L}^1:\text{L}^2 = (16.0/4):2.5 = 1.6:1$
LIFM-51	$\text{L}^1:\text{L}^3 = 4:1$	$\text{L}^1:\text{L}^3 = (8.0/2):(3.56/4) = 4.3:1$
LIFM-52	---	$\text{L}^1:\text{L}^4 = (16.0/4):3.5 = 1.1:1$
LIFM-53	$\text{L}^1:\text{L}^5 = 4:1$	$\text{L}^1:\text{L}^5 = (8.0/2):(1.76/2) = 4.5:1$

<sup>a</sup> Based on integral area of corresponding H peaks.

## S9. $\text{N}_2$ Sorption Isotherm

Before gas sorption experiments, All as-synthesized samples were washed with *N,N*-dimethylformamide (DMF) and immersed in anhydrous methanol for 3 days, and then immersed in anhydrous dichloromethane for another 3 days, during which the solvent was decanted and freshly replenished three times a day. All the samples were activated under vacuum at 100 °C for 10 hours. Gas sorption measurements were then conducted using a quantachrome autosorb-iQ2-MP gas adsorption analyzer.

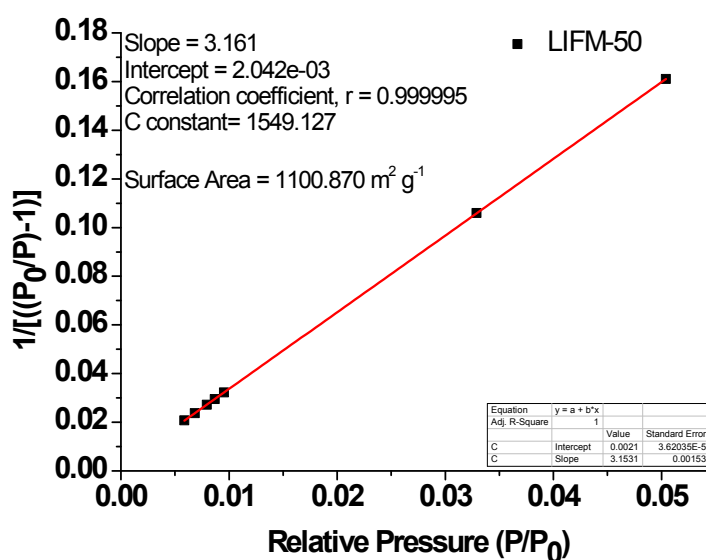


**Figure S18** Plot of the linear region on the  $\text{N}_2$  isotherm of LIFM-50 for the BET equation.

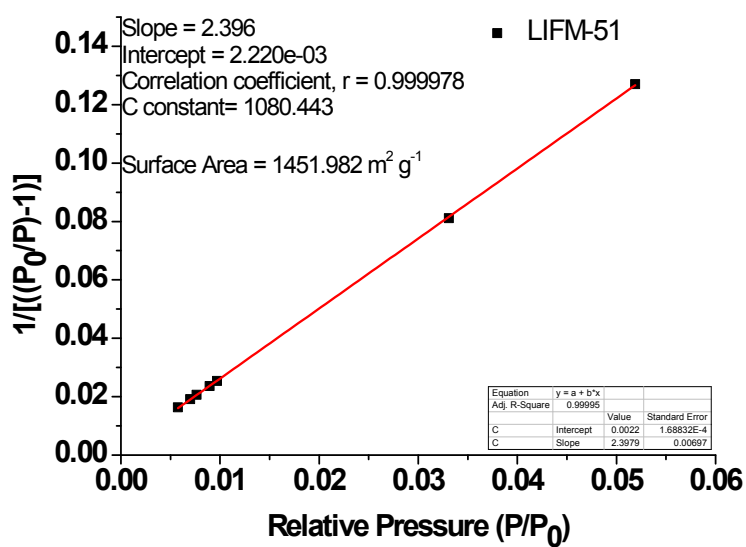


**Figure S19** Plot of the linear region on the N<sub>2</sub> isotherm of LIFM-51 for the BET equation.

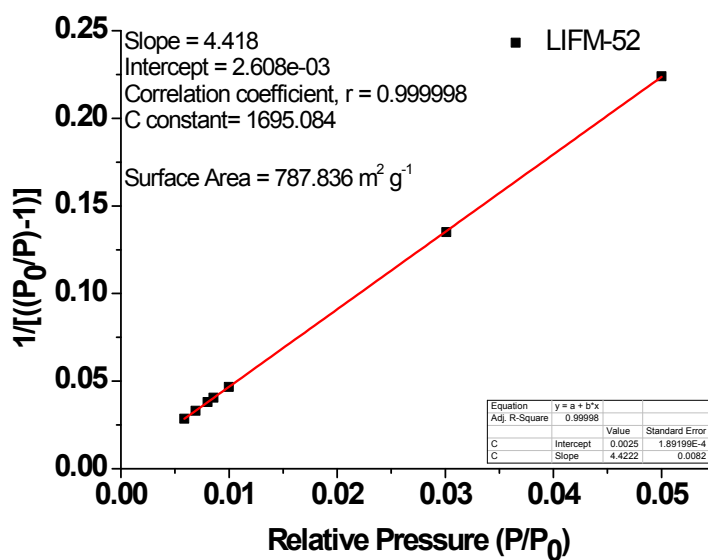


**Figure S20** Plot of the linear region on the N<sub>2</sub> isotherm of LIFM-52 for the BET equation.

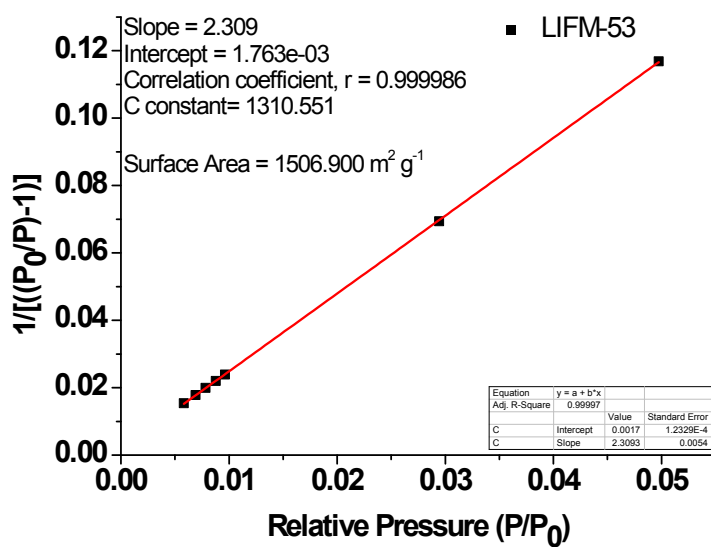


**Figure S21** Plot of the linear region on the N<sub>2</sub> isotherm of LIFM-53 for the BET equation.

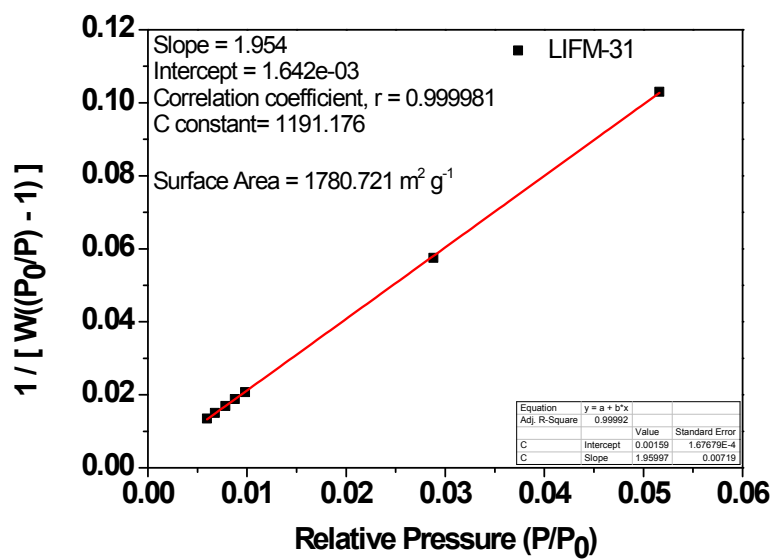


**Figure S22** Plot of the linear region on the N<sub>2</sub> isotherm of LIFM-31 for the BET equation.

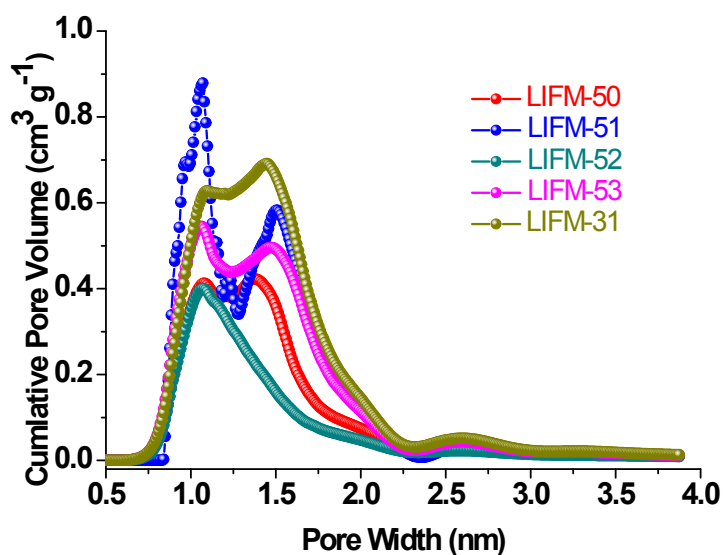


**Figure S23** Pore size distribution of LIFM-50, LIFM-51, LIFM-52, LIFM-53 and LIFM-31 calculated from SF analysis.

**Table S3** Summary of porosity parameters of LIFM-50, LIFM-51, LIFM-52, LIFM-53 and LIFM-31.

Structure	$S_{\text{BET}}$ ( $\text{m}^2/\text{g}$ )	Total Pore Volume ( $\text{cc/g}$ )	Pore Size by SF ( $\text{\AA}$ )
LIFM-50	1100	0.46	10.8, 13.8
LIFM-51	1451	0.59	10.7, 15.0
LIFM-52	787	0.36	11.7
LIFM-53	1506	0.63	11.6, 14.6
LIFM-31	1780	0.73	11.0, 14.5

## S10. Dynamic Reversible Ligand Installation

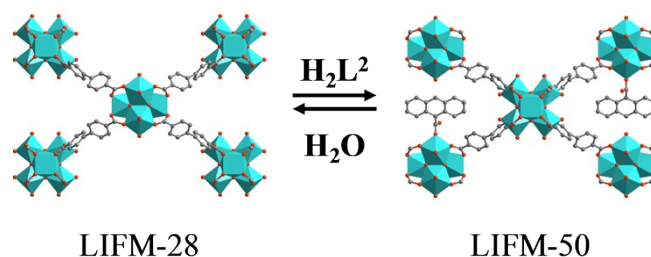
Dynamic reversible installation process has been performed as following with LIFM-50 as representative:

**From LIFM-50 to LIFM-28 (Scheme S3):** LIFM-50 (~ 30 mg) was soaked in 10.0 mL pH = 10 aqueous solution for 3 days under room temperature, during which the aqueous solution was decanted and freshly replenished three times a day. Then the mixture was centrifuged to obtain the solid. Afterwards, the samples were washed thoroughly with  $\text{H}_2\text{O}$  (10 mL $\times$ 3), pH = 10 aqueous solution in DMF (10mL $\times$ 3) and DMF solution (10mL $\times$ 3), and dried naturally. The samples were characterized by

powder X-ray diffraction (Figure S24). In order to confirm whether the disassembled spacers have been efficiently removed, part of the samples were digested with sonication in 490  $\mu\text{L}$  DMSO- $d_6$  and 10  $\mu\text{L}$   $\text{D}_2\text{SO}_4$  for  $^1\text{H}$  NMR analysis (Figure S25). The rest of the above samples were left to soak in DMF for the following step.

**From LIFM-28 to LIFM-50:**  $\text{H}_2\text{L}^2$  (10.0 mg) was dissolved in 2.0 mL DMF with sonication, then the rest samples (around 10 mg) were introduced into the  $\text{H}_2\text{L}^2$  solution, followed by incubating the mixture in an isothermal oven at 75  $^\circ\text{C}$  for 30 h. After cooling, the mixture was centrifuged, dried naturally. And the samples were characterized by powder X-ray diffraction (Figure S24).

### 10.1 The Reversible Installation between LIFM-50 and LIFM-28 :



**Scheme S3** The reversible installation between LIFM-28 and LIFM-50.

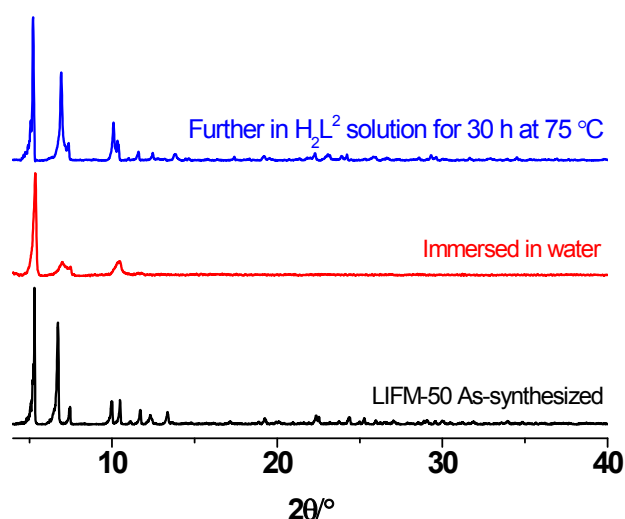


**Figure S24** The PXRD patterns of reversible installation process between LIFM-28 and LIFM-50.



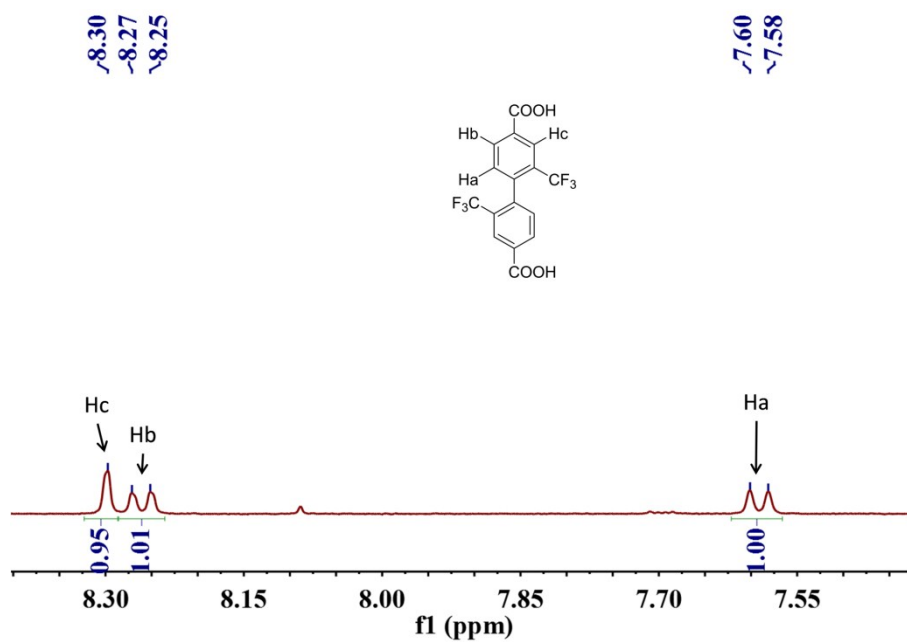
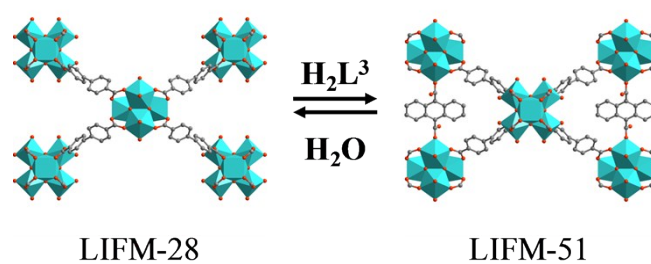


**Figure S25**  $^1\text{H}$  NMR spectroscopy of digested LIFM-28 which has been recovered from LIFM-50 by soaking in water.

## 10.2 The Reversible Installation between LIFM-51 and LIFM-28 :



**Scheme S4** The reversible installation between LIFM-28 and LIFM-51.

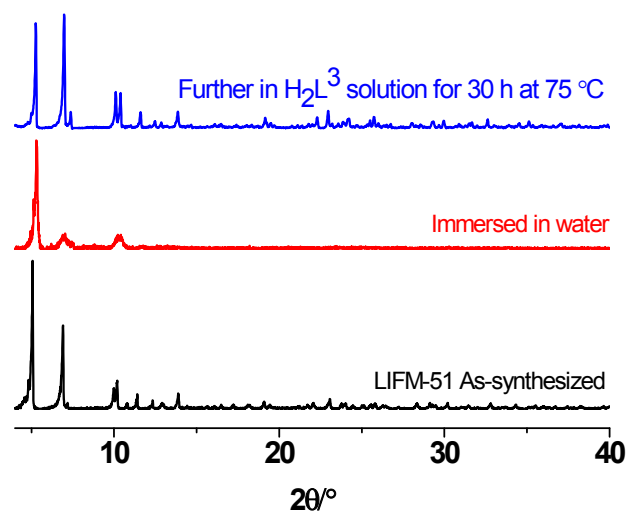


**Figure S26** The PXRD patterns of reversible installation process between LIFM-28 and LIFM-51.

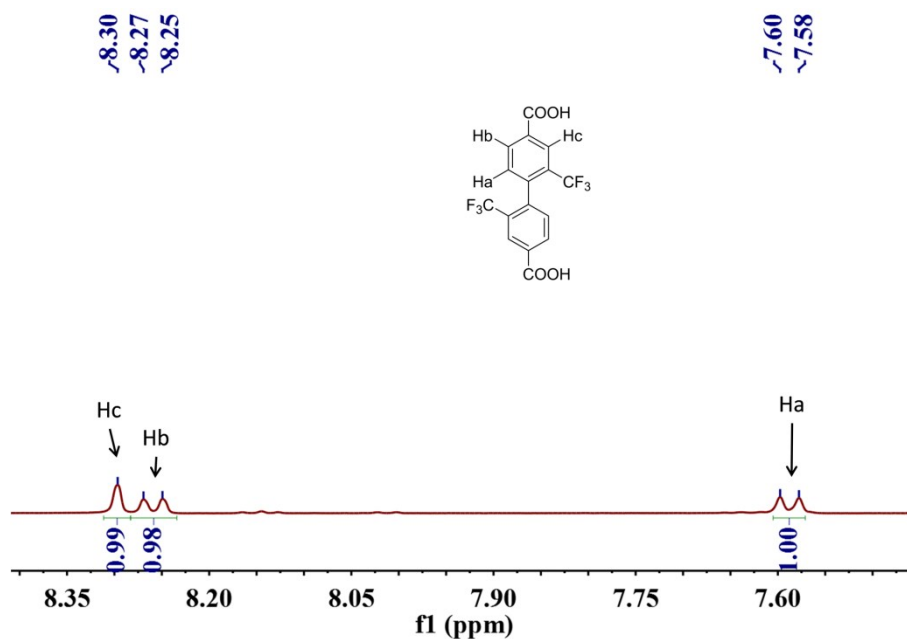
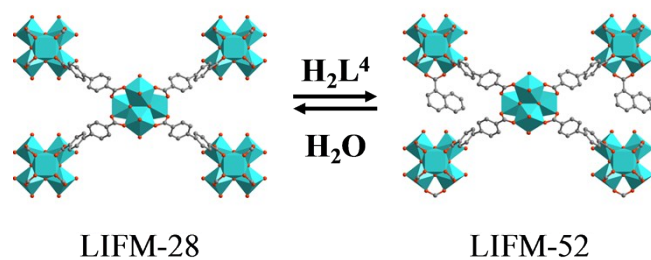


**Figure S27**  $^1\text{H}$  NMR spectroscopy of digested LIFM-28 which has been recovered from LIFM-51 by soaking in water.

### 10.3 The Reversible Installation between LIFM-52 and LIFM-28 :



**Scheme S5** The reversible installation between LIFM-28 and LIFM-52.

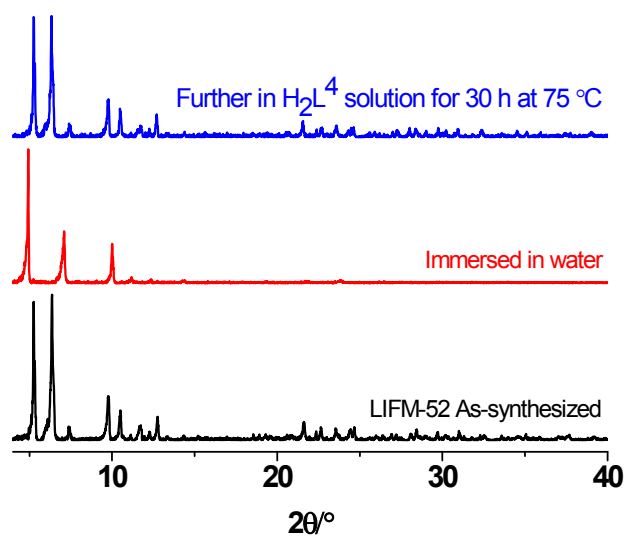


**Figure S28** The PXRD patterns of reversible installation process between LIFM-28 and LIFM-52.

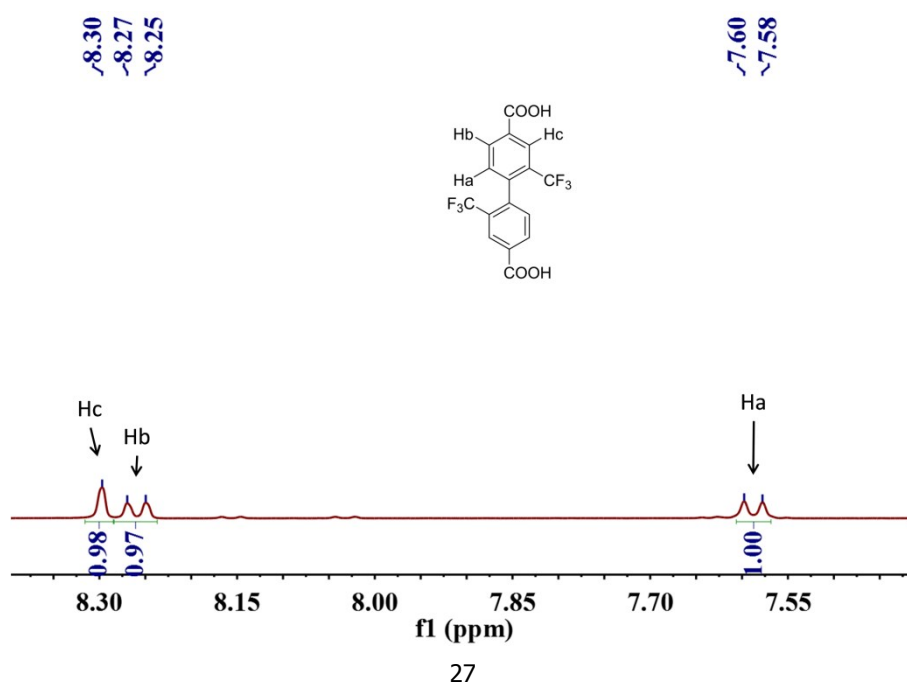
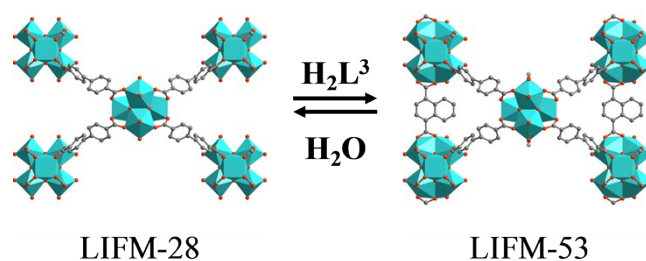


**Figure S29**  $^1\text{H}$  NMR spectroscopy of digested LIFM-28 which has been recovered from LIFM-52 by soaking in water.

#### 10.4 The Reversible Installation between LIFM-53 and LIFM-28 :



**Scheme S6** The reversible installation between LIFM-28 and LIFM-53.

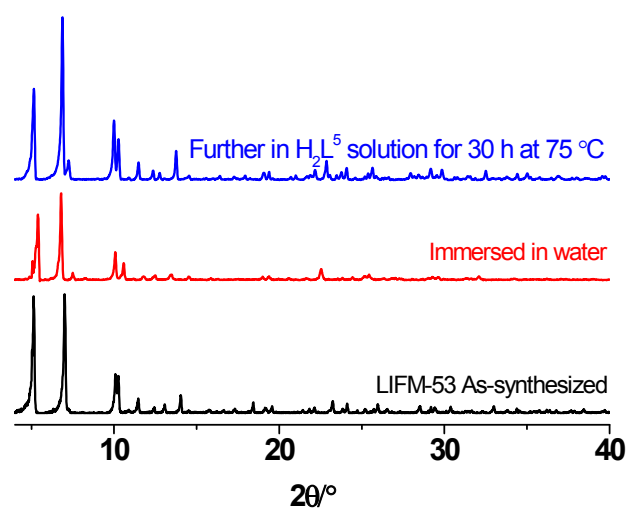


**Figure S30** The PXRD patterns of reversible installation process between LIFM-28 and LIFM-53.

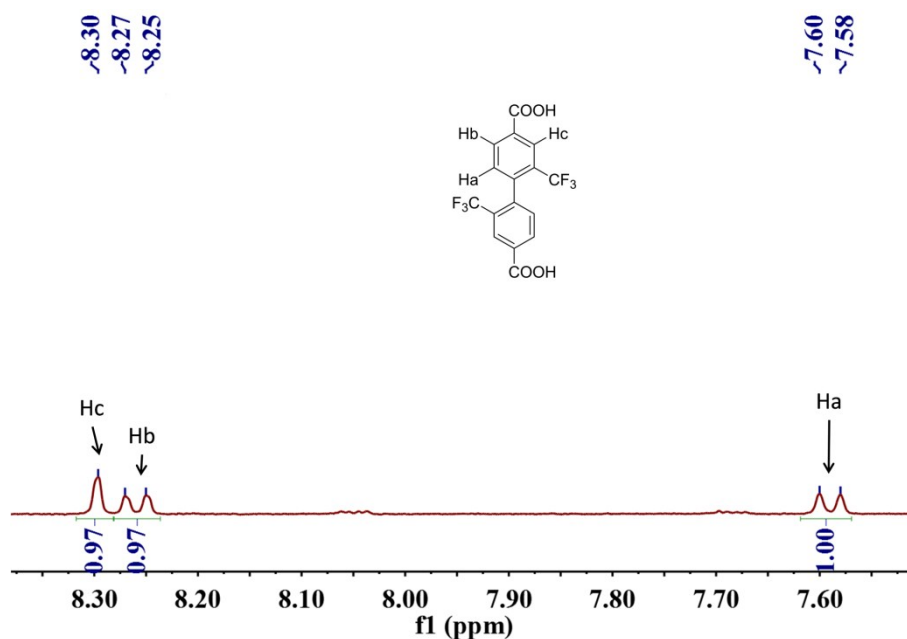
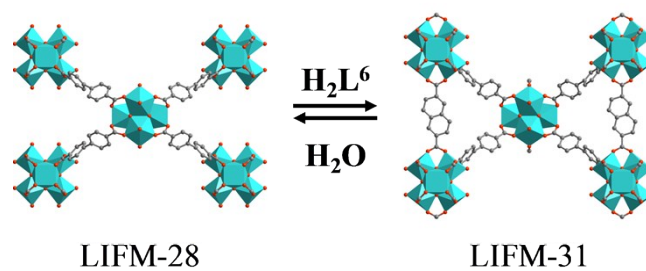


**Figure S31**  $^1\text{H}$  NMR spectroscopy of digested LIFM-28 which has been recovered from LIFM-53 by soaking in water.

#### 10.5 The Reversible Installation between LIFM-31 and LIFM-28 :



**Scheme S7** The reversible installation between LIFM-28 and LIFM-31.

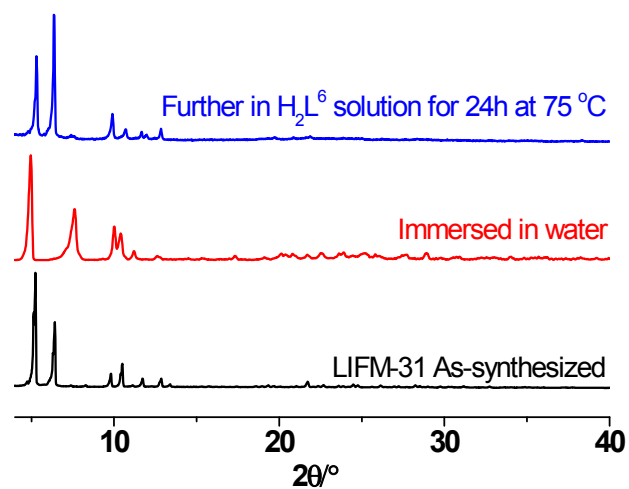


**Figure S32** The PXRD patterns of reversible installation process between LIFM-28 and LIFM-31.

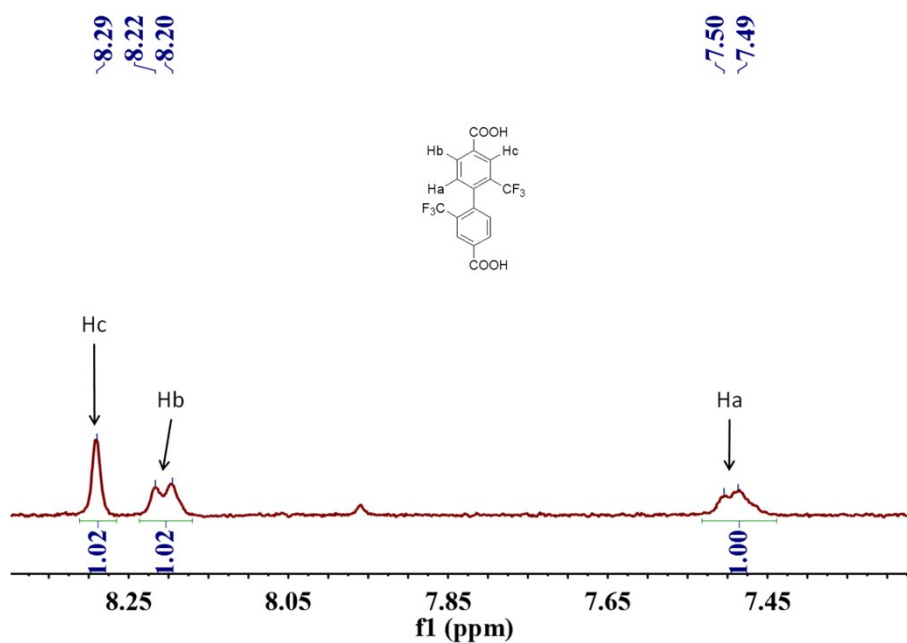


**Figure S33**  $^1\text{H}$  NMR spectroscopy of digested LIFM-28 which has been recovered from LIFM-31 by soaking in water.

## S11. Microscopic Photos

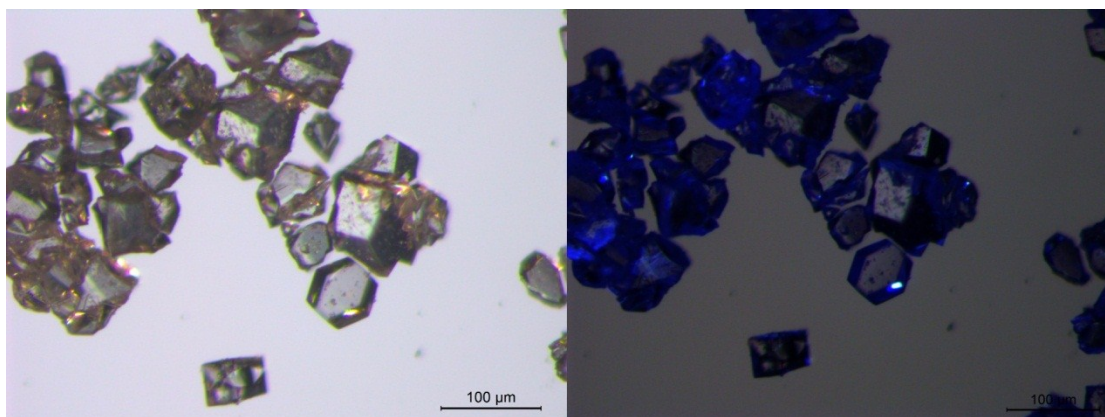


**Figure S34** Microscopic photos of LIFM-28 under daylight (left) and UV light (right).

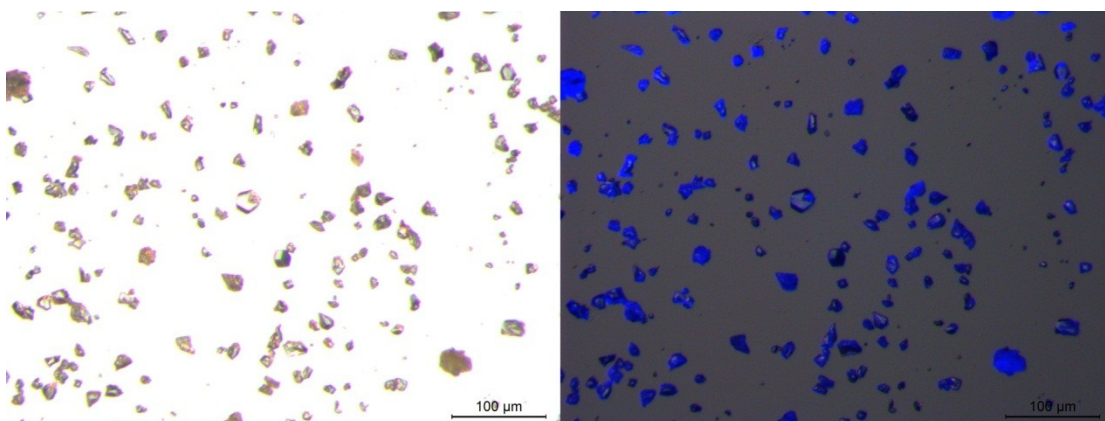


**Figure S35** Microscopic photos of LIFM-50 under daylight (left) and UV light (right).

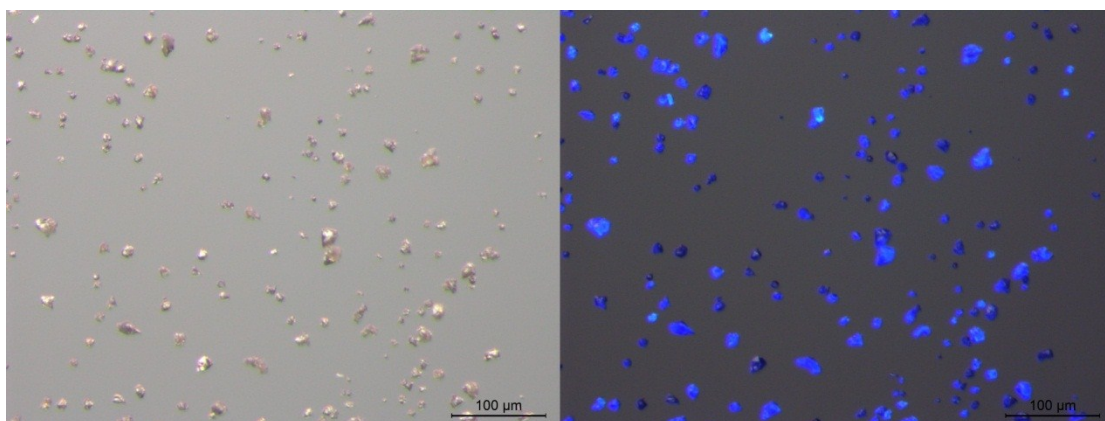


**Figure S36** Microscopic photos of LIFM-51 under daylight (left) and UV light (right).



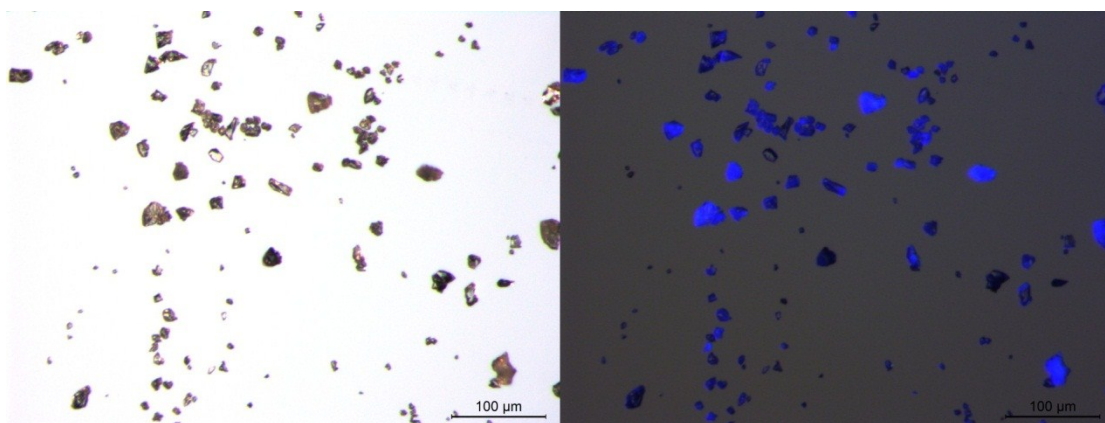


**Figure S37** Microscopic photos of LIFM-52 under daylight (left) and UV light (right).

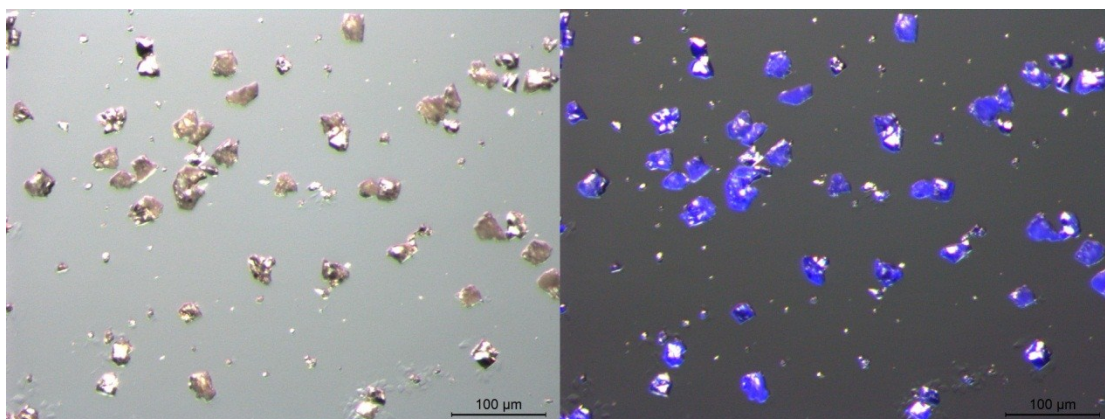


**Figure S38** Microscopic photos of LIFM-53 under daylight (left) and UV light (right).

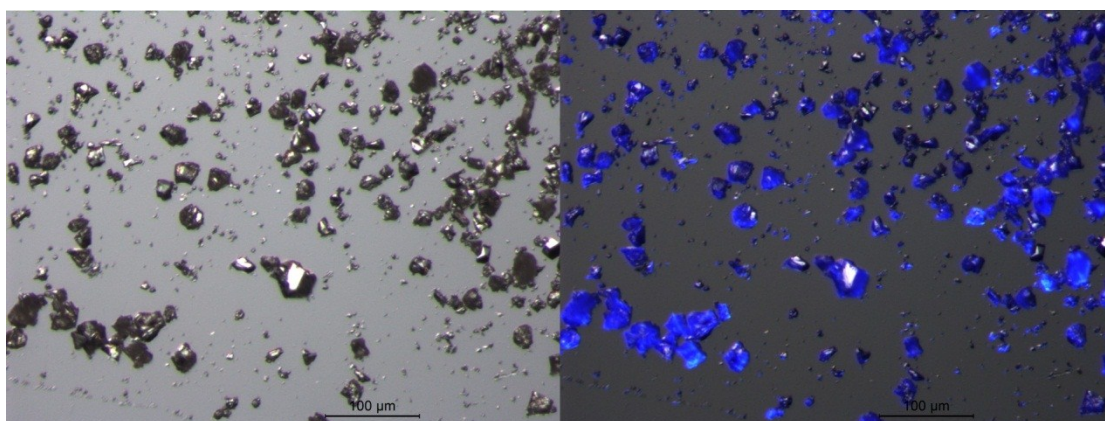


**Figure S39** Microscopic photos of LIFM-31 under daylight (left) and UV light (right).



## S12. PXRD, UV-Vis Spectra and Fluorescent Spectra of Reinstalled MOFs

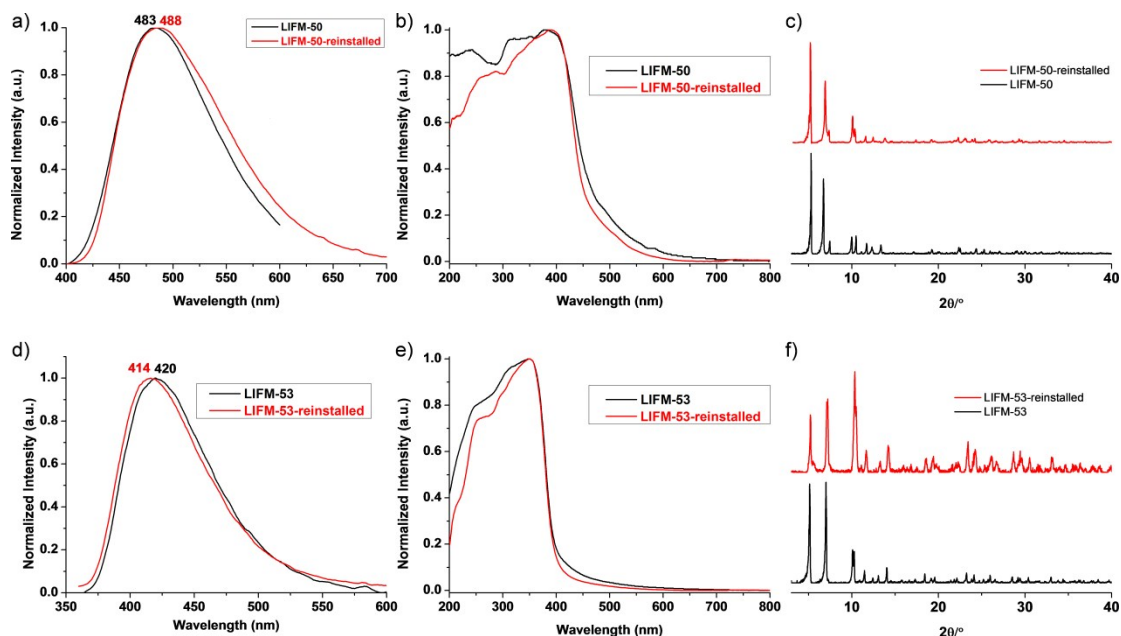


**Figure S40** The fluorescent spectra (a & d), UV-Vis absorption spectra (b & e) and PXRD patterns (c & f) of LIFM-50 and LIFM-53, respectively.

## S13. Reference

1. C.-X. Chen, Z. Wei, J.-J. Jiang, Y.-Z. Fan, S.-P. Zheng, C.-C. Cao, Y.-H. Li, D. Fenske and C.-Y. Su, *Angew. Chem. Int. Ed.*, 2016, **55**, 9932-9936.
2. Quah, H. S.; Ng, L. T.; Donnadieu, B.; Tan, G. K.; Vittal, J. J. *Inorg. Chem.* **2016**, *55*, 10851-10854.
3. G. Sheldrick, *Acta Crystallogr. A*, 2008, **64**, 112-122.
4. L. Spek, *Acta Crystallogr. C*, 2015, **71**, 9-18.